PtP_2 nanoparticles on N, P doped carbon with self-converting process to core-shell Pt/PtP_2 as efficient and robust ORR catalyst

Wu Tian,[a] Yanwei Wang,[a] Weiwei Fu,[a] Jinfeng Su,[a] Han Zhang[b*], Yu Wang [a,b*]

[a]The School of Chemistry and Chemical Engineering, State Key Laboratory of Power Transmission Equipment & System Security and New Technology, Chongqing University, 174 Shazheng Street, Shapingba District.

[b]The School of Electrical Engineering, Chongqing University, 174 Shazheng Street, Shapingba District, Chongqing City, 400044, P.R. China.

*E-mail: wangy@cqu.edu.cn; hanzhang@cqu.edu.cn

Theoretical details

Calculations details of the Oxygen Reduction Reaction

In the acidic solution, the overall ORR reaction is:

$$O_2 + 4H^+ + 4e^- \rightarrow 2H_2O$$

The ORR can proceed through the following elementary steps usually employed to investigate the electrocatalysis of the ORR on various materials:

$$R1: O_2\,(g) + H^+ + e^- + * \rightarrow *OOH$$

$$R2: *OOH + H^+ + e^- \rightarrow *O + H_2O\,(l)$$

$$R3: *O + H^+ + e^- \rightarrow *OH$$

$$R4: *OH + H^+ + e^- \rightarrow H_2O\,(l) + *$$

where * represents an active site on the catalytic surface, and (l) and (g) refer to the liquid and gas phase, respectively.

According to previous studies,[1, 2] the Gibbs free energy of each step is calculated as follows (equation 1):

$$\Delta G = \Delta E + \Delta ZPE - T\Delta S$$

Where the ΔE can be obtained by the computation of geometrical structures, ΔZPE is the difference in zero point energies due to the reaction, and the ΔS is the change in

entropy calculated using vibrational frequencies analysis.

Experimental details

Electrochemically active surface area (ESCA)

Cyclic voltammetry (CV) measurements were carried out in 0.1 M $HClO_4$ solutions under a flow of Ar (Airgas, ultrahigh purity) at a sweep rate of 50 mV/s. The ECSA was estimated by measuring the charge associated with Hupd adsorption (QH) between 0 and 0.37 V and assuming 210 μC/cm^2 for the adsorption of a monolayer of hydrogen on a Pt surface (q_H). The H_{upd} adsorption charge (QH) can be determined using QH = 0.5 × Q, where Q is the charge in the H_{upd} adsorption/desorption area obtained after double-layer correction. Then, the specific ECSA was calculated based on the following relation:[3]

$$\text{specific ECSA} = \frac{Q_H}{m * q_H}$$

where QH is the charge for H_{upd} adsorption, m is the loading amount of metal, and q_H is the charge required for monolayer adsorption of hydrogen on a Pt surface.

Number of electron transfer

As for ORR experiment, O_2 was bubbled for 20 min prior to the test and maintained in the headspace of the electrolyte throughout the testing process. The working electrode was scanned cathodically at a rate of 10 mV s^{-1} with varying rotating speed from 400 to 2000 rpm in O_2 -saturated 0.1 M $HClO_4$ aqueous solution. The electron transfer number per oxygen molecule for oxygen reduction can be determined on the basis of the Koutechy-Levich equations:[4]

$$1/J = 1/J_L + 1/J_K = 1/B\omega^{1/2} + 1/J_K \qquad (1)$$

$$B = 0.62nFC_0 (D0)^{2/3} \nu^{-1/6} \qquad (2)$$

$$J_K = nFkC_0 \qquad (3)$$

Where J is the measured current density and is the electrode rotating rate (rad s^{-1}). B is determined from the slope of the Koutechy-Levich (K-L) plot based on Levich equation

(2). J_L and J_K are the diffusion and kinetic-limiting current densities, n is the transferred electron number, F is the Faraday constant (F= 96485 C mol^{-1}), C_0 is the O_2 concentration in the electrolyte (C_0 = 1.26×10^{-6} mol cm^{-3}), D_0 is the diffusion coefficient of O_2 (D_0 = 1.93×10^{-5} cm^2 s^{-1}), and v is the kinetic viscosity (v = 0.01009 cm^2 s^{-1}). The constant 0.62 is adopted when the rotation speed is expressed in rad s^{-1}. For ORR experiments, the LSV curves were obtained at a scan rate of 10 mV s^{-1}. In order to obtain a stable current, the LSV data were collected at the second sweep.

Mass and specific activities

The ORR measurements were performed in 0.1 M $HClO_4$ solutions under flow of O_2 (Airgas, Research grade) using the glassy carbon RDE at a rotation rate of 1,600 rpm and a sweep rate of 10 mV/s. In order to produce a clean electrode surface, several potential sweeps between -0.05 and 1.3 V versus RHE were applied to the electrode prior to the ORR measurement. In the ORR polarization curve, current densities were normalized in reference to the geometric area of the glassy carbon RDE (0.196 cm^2).

For the ORR at a RDE, the Koutecky-Levich equation can be described as follows:

$$\frac{1}{i} = \frac{1}{i_k} + \frac{1}{i_d}$$

Where i is the experimentally measured current, i_d is the diffusion-limiting current, and i_k is the kinetic current. Then, the kinetic current was calculated based on the following equation:

$$i_k = \frac{i * i_d}{i_d - i}$$

For each catalyst, the kinetic current was normalized to loading amount of metal and ECSA in order to obtain mass and specific activities, respectively. The accelerated durability tests were performed at room temperature in O_2-saturated 0.1 M $HClO_4$ solutions by applying cyclic potential sweeps between 0.3 and 1.3 V versus RHE at a sweep rate of 50 mV/s for a given number of cycles.

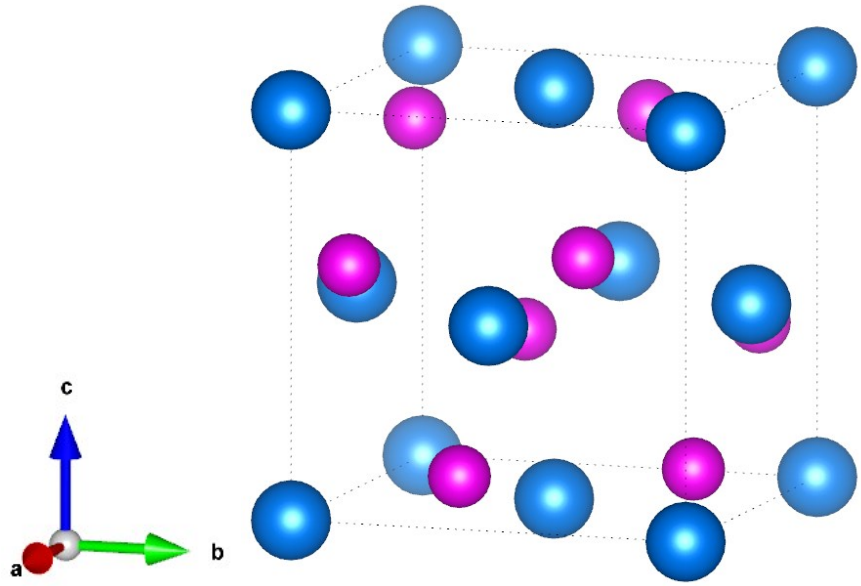

Figure S1. Optimized bulk PtP_2 model. Atom colors: blue: Pt, purple: P.

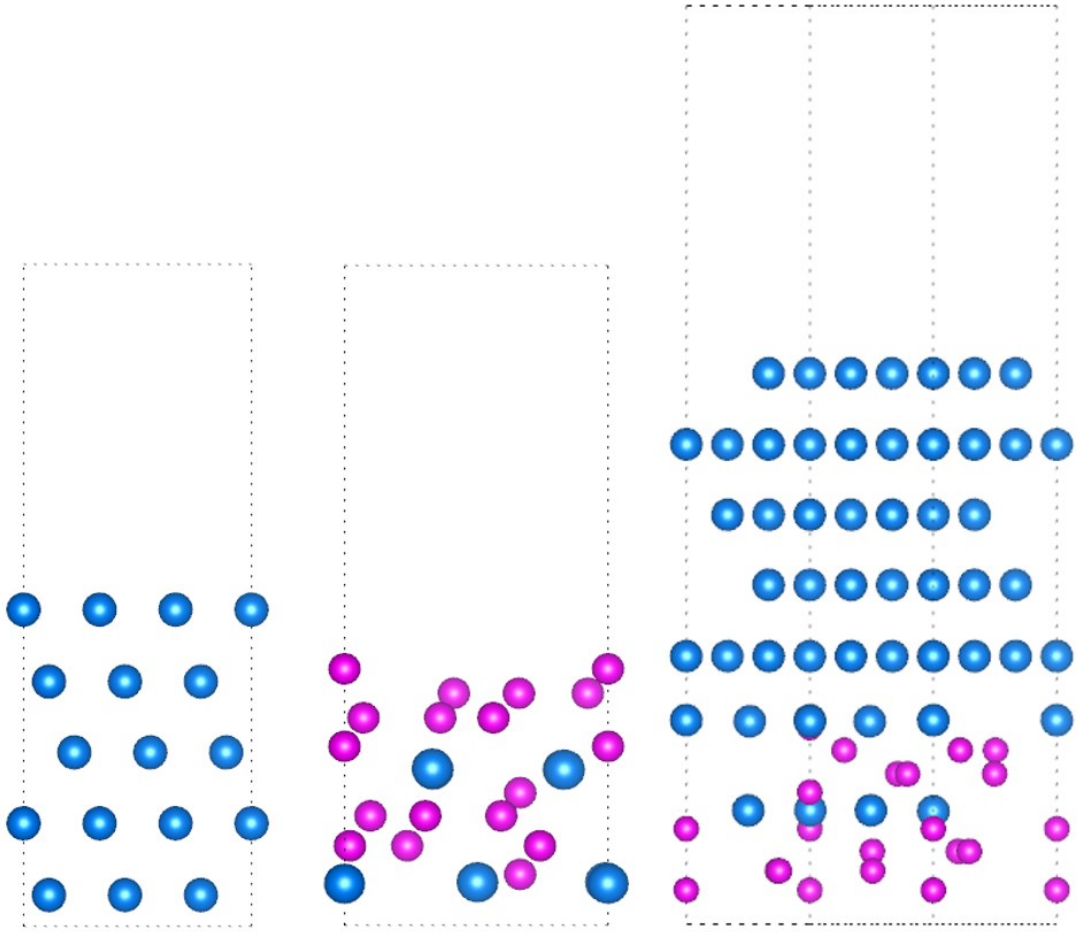

Figure S2. The theoretical models used in DFT calculations of Pt (111), PtP_2 (111) and Pt/PtP_2 (111), respectively. Atom colors: blue: Pt, purple: P.

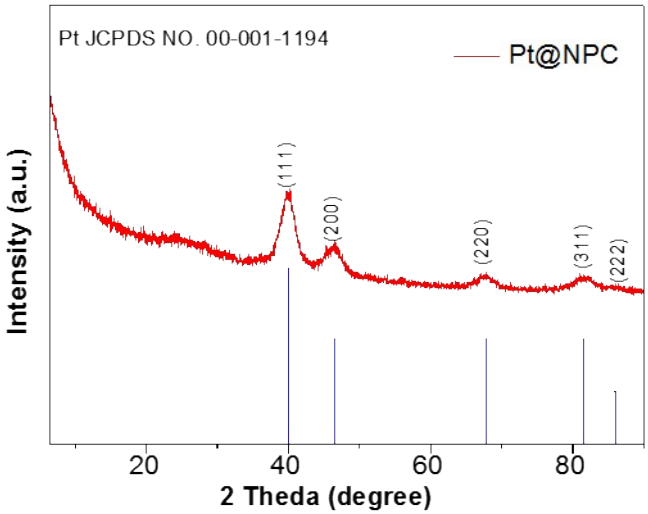

Figure S3. XRD pattern of as-synthesized Pt@NPC.

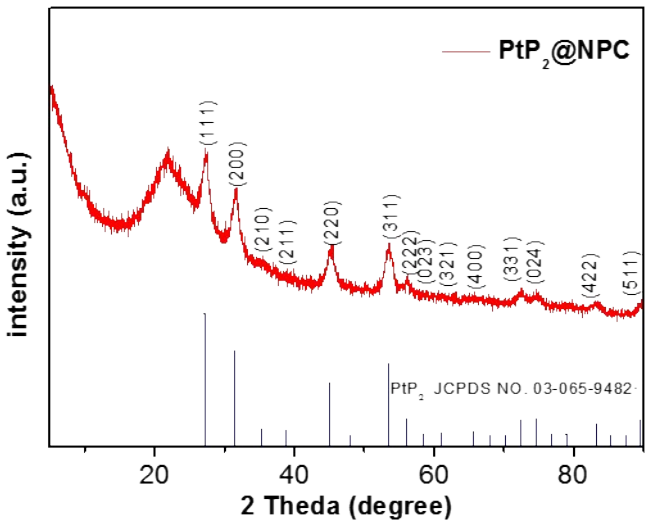

Figure S4. XRD pattern of synthesized PtP_2@NPC before etching process of SiO_2 template. The residual peaks can be assigned to SiO_2.

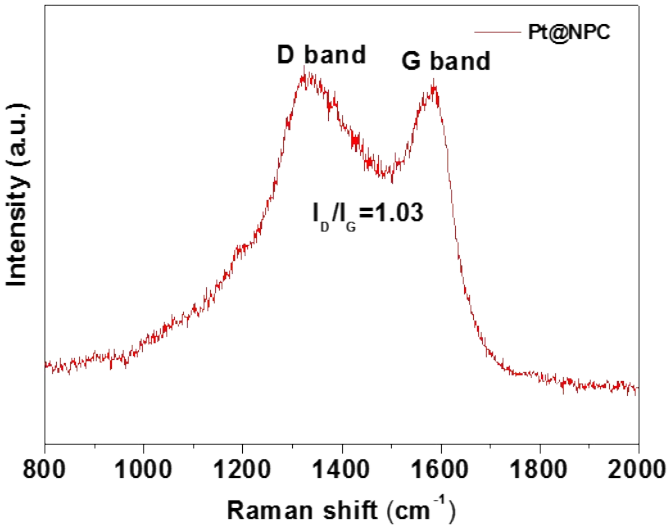

Figure S5. Raman spectrum of Pt @NPC.

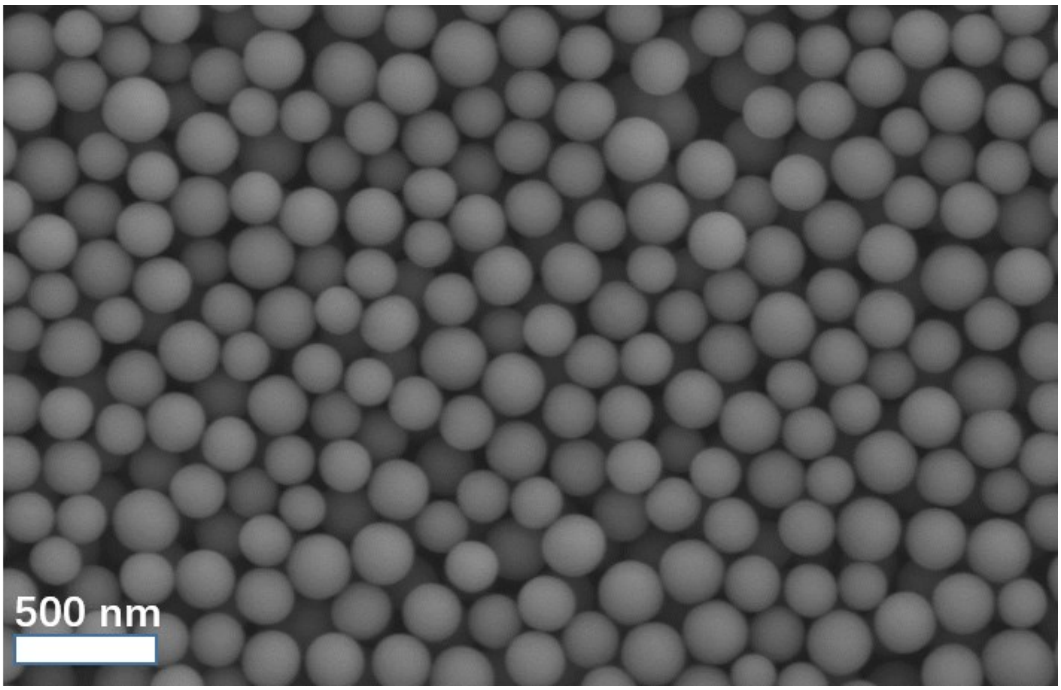

Figure S6. SEM image of the synthesized SiO_2 spheres.

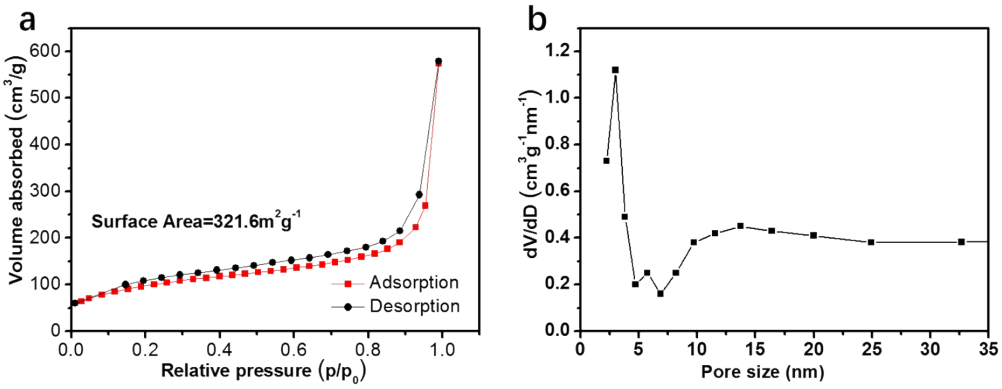

Figure S7. （a） Nitrogen absorption/desorption curve and （b） the pore size distribution of PtP_2@NPC with using of SiO_2 spheres as template.

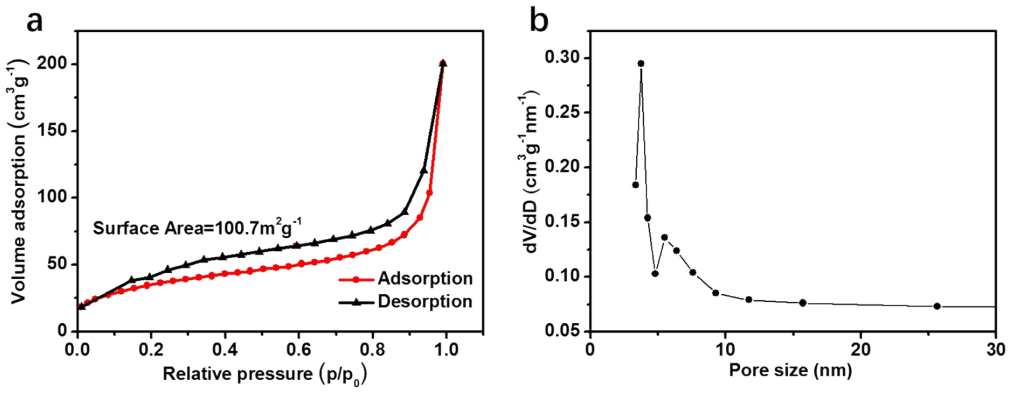

Figure S8. （a） Nitrogen absorption/desorption curve and （b） the pore size distribution of PtP_2@NPC without using of SiO_2 spheres as template.

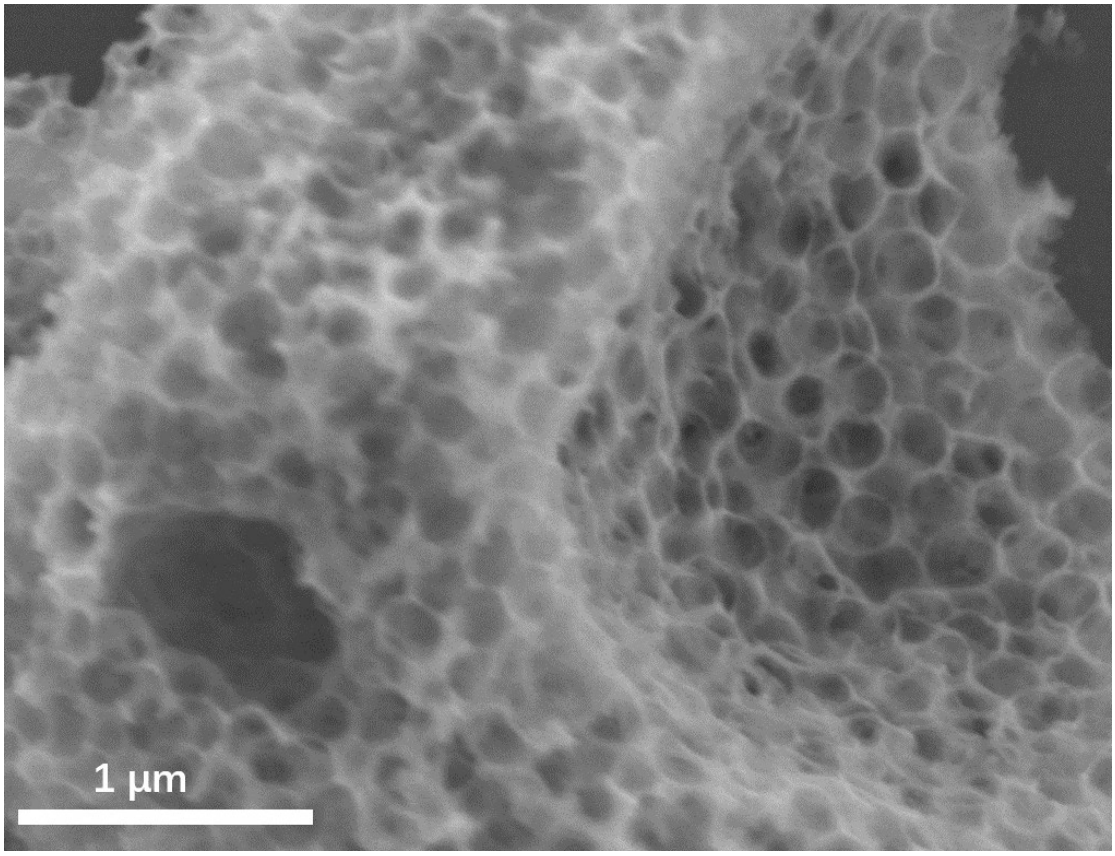

Figure S9. SEM image of Pt/PtP_2@NPC after etching of SiO_2 template.

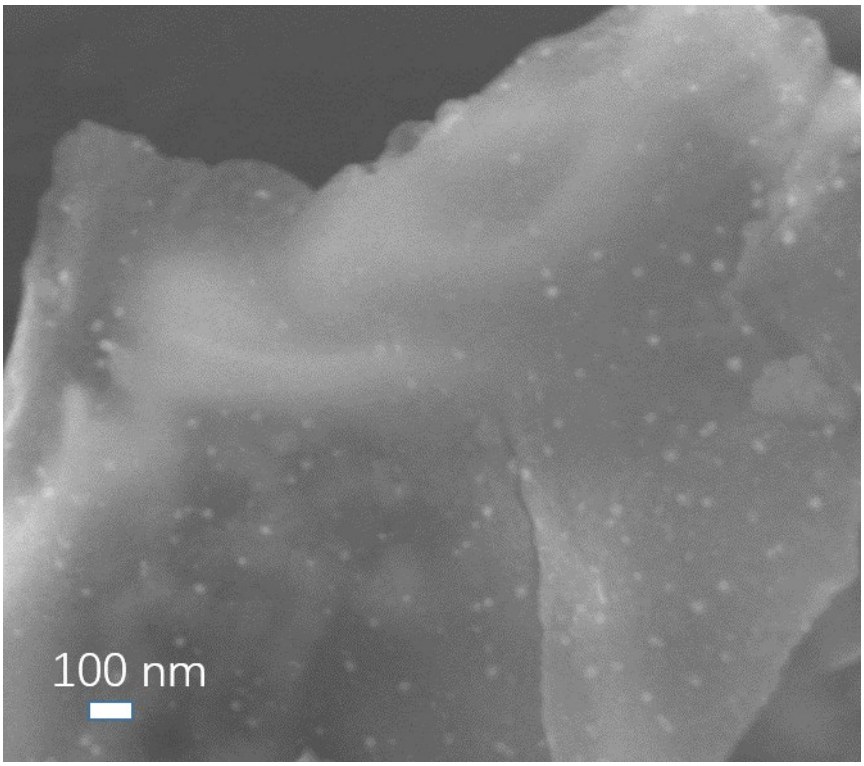

Figure S10. SEM image of PtP_2@NPC without using SiO_2 as template. We can see the solid and aggregated morphology of the carbon support.

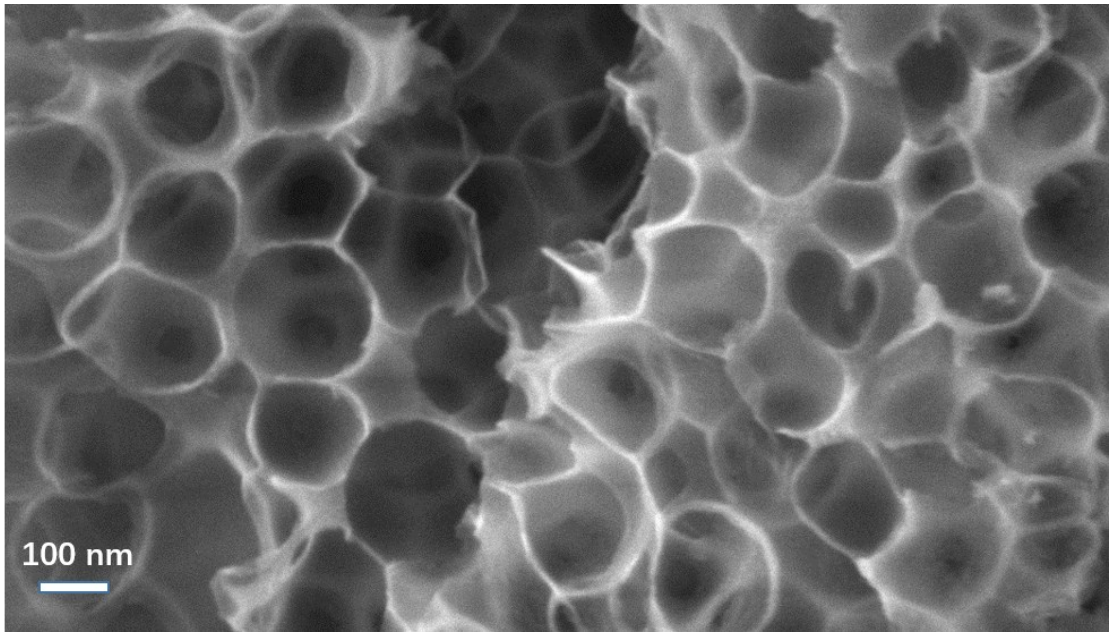

Figure S11. SEM image of bubble-like carbon framework after stability test. No deformation after reaction confirms stability of the porous morphology.

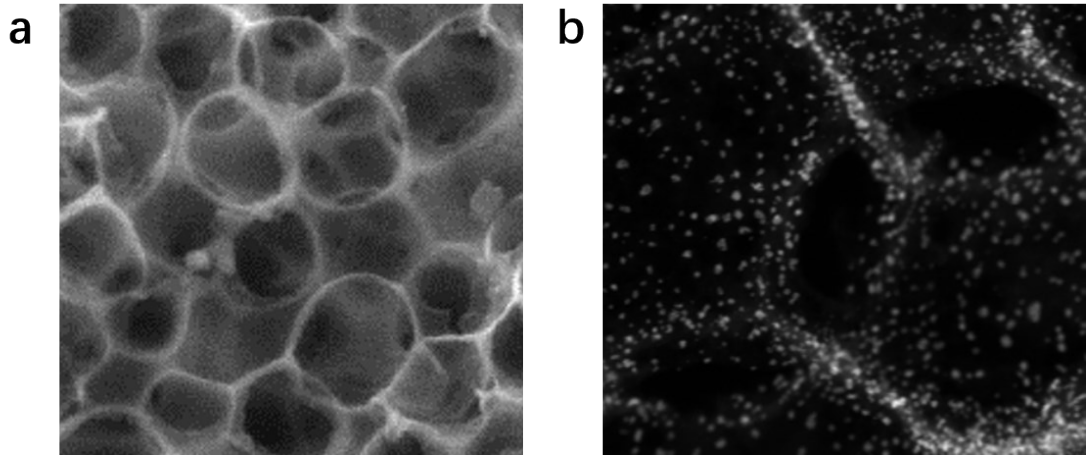

Figure S12. (a) and (b) magnified SEM or HAADF-STEM image of PtP_2@NPC after etching of SiO_2 template

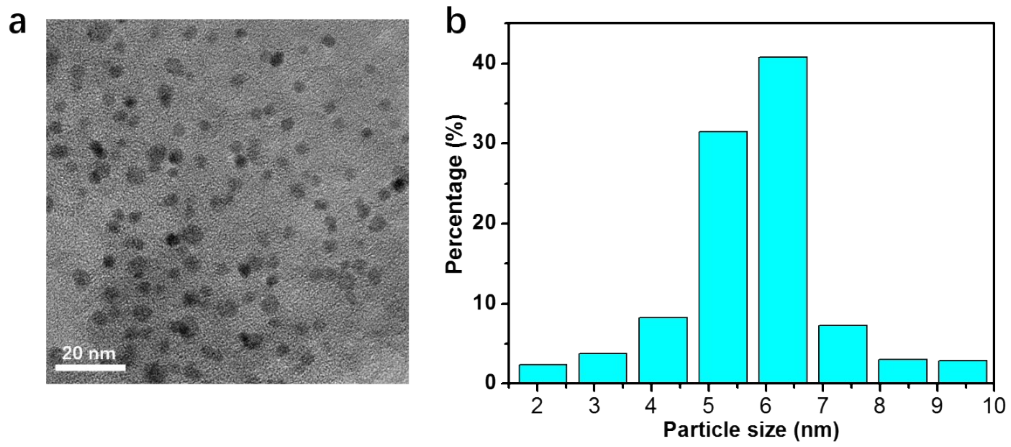

Figure S13. SEM image and corresponding particle size distribution plot of Pt/PtP_2 NPs.

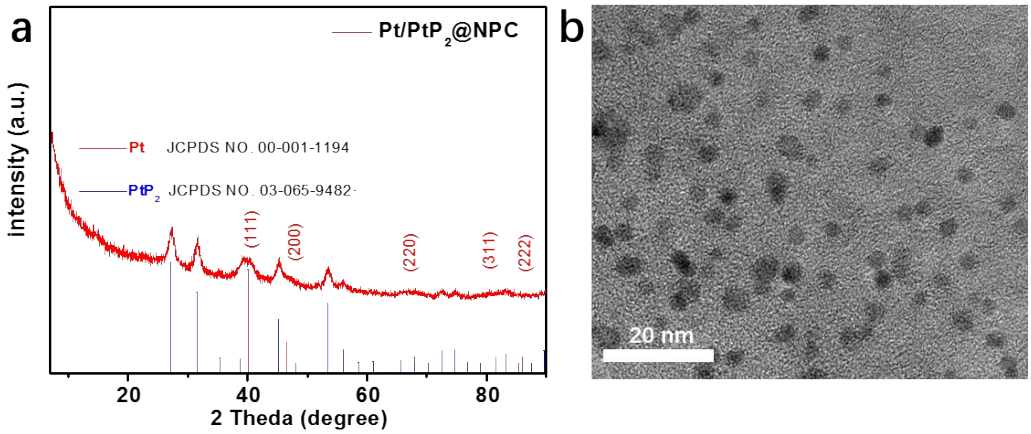

Figure S14. XRD data (a) and TEM image (b) of Pt/PtP_2 after durability test

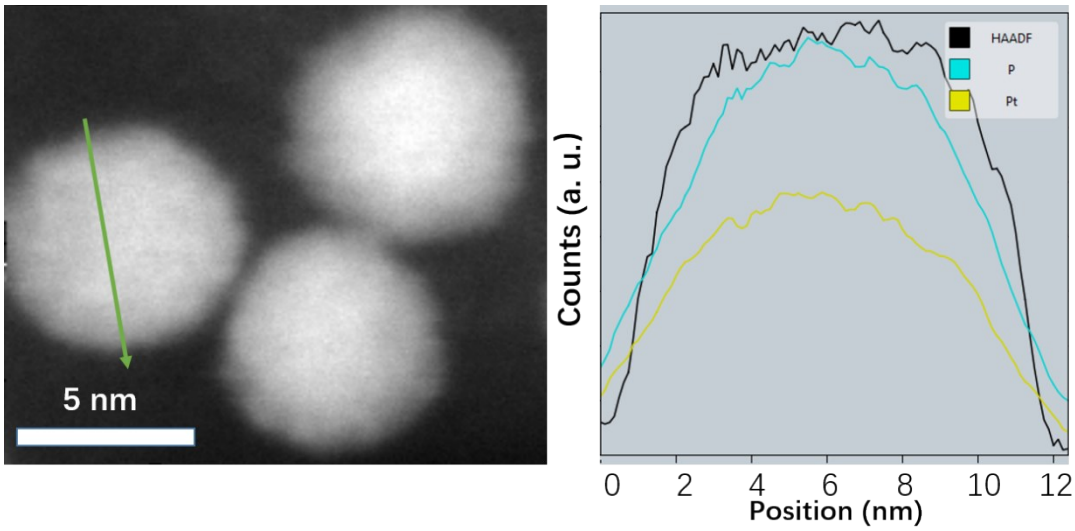

Figure S15. （a）HAADF-STEM imaging of a representative as-synthesized PtP_2@NPC. (b) STEM line scans crossing the representative as-synthesized PtP_2@NPC.

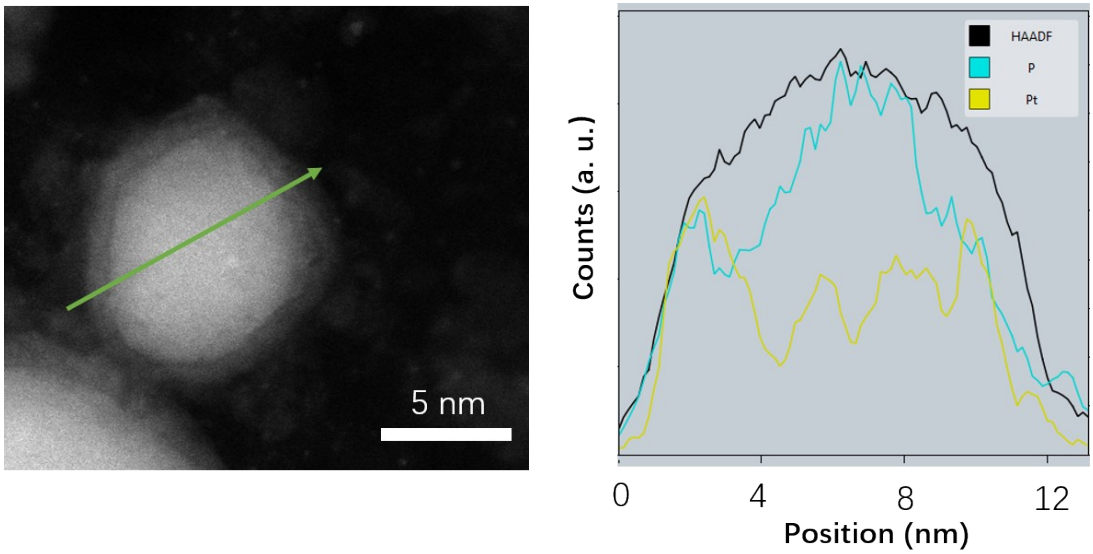

Figure S16. （a）HAADF-STEM imaging of a representative as-synthesized Pt/PtP_2@NPC. (b) STEM line scans crossing the representative as-synthesized Pt/PtP_2@NPC. We can see that Pt content on the surface area (approximately 1 nm) of Pt/PtP_2 is comparatively higher than that of PtP_2 counterpart, confirming the surface concentration of Pt on the surface.

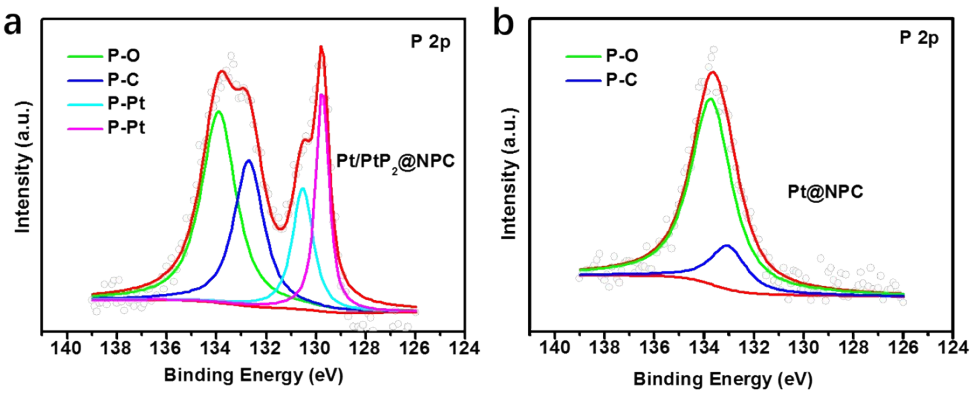

Figure S17. XPS spectra of P (2p) of Pt/PtP_2@NPC (a) and Pt@NPC (b).

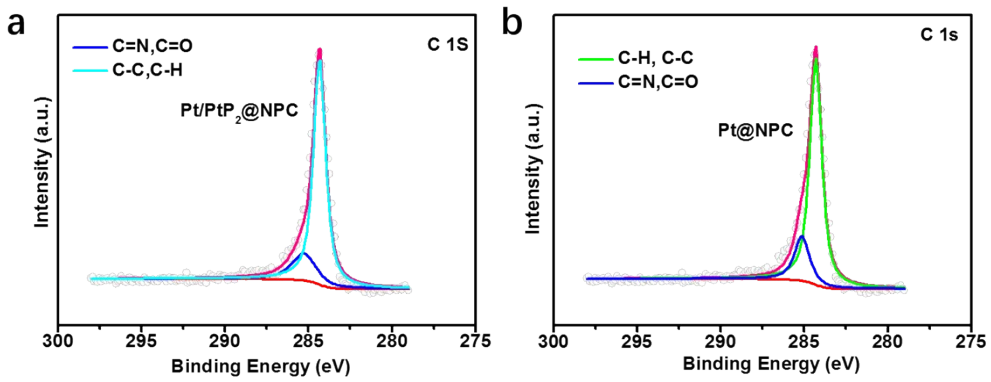

Figure S18. XPS spectra of C (1s) of Pt/PtP_2@NPC (a) and Pt@NPC (b).

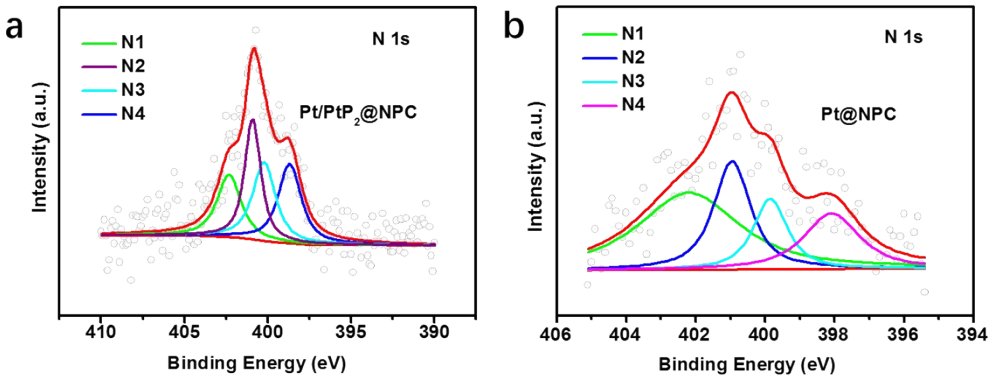

Figure S19. XPS spectra of N (1s) of Pt/PtP_2@NPC (a) and Pt@NPC (b).

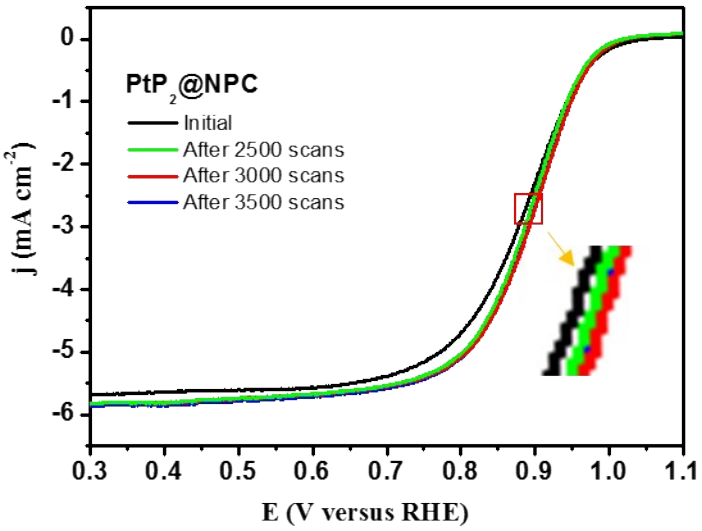

Figure S20. LSV curves of PtP_2 at initial, 2000, 3000 and 4000 circles.

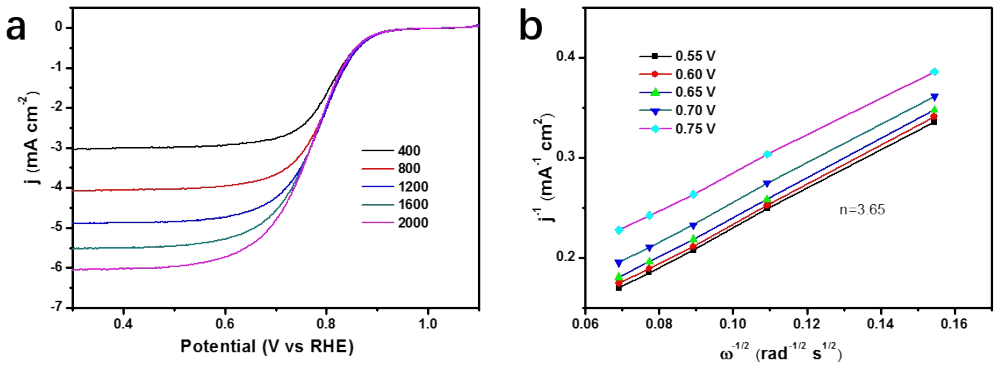

Figure S21. LSV curves of NPC at 400, 800, 1200, 1600 and 2000 rpm with a sweep rate of 10 mV s^{-1} in O_2-saturated 0.1 M $HClO_4$ solutions. (c) K–L plots of NPC at the potential of 0.55, 0.60, 0.65, 0.70 and 0.75 V (n = 3.65).

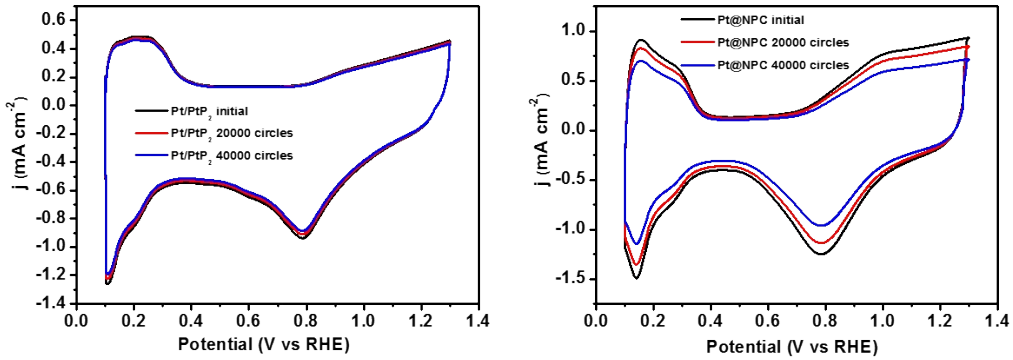

Figure S22. CV curves of Pt/PtP_2@NPC and Pt@NPC before and after different potential cycles.

Table S1. Comparison of ORR parameters for the Pt@NPC, PtP_2@NPC, Pt/PtP_2@NPC and commercial Pt/C catalyst in 0.1M $HClO_4$.

Sample	E_{half} (V vs RHE)	$j_{ECSA,0.90V}$ (mA cm^{-2})	$j_{mass,0.90V}$ (A mg^{-1}_{Pt})	ECSA (m^2 g^{-1})
Pt@NPC	0.872	0.178	0.149	83.89
PtP_2@NPC	0.883	0.438	0.466	106.43
Pt/PtP_2@NPC	0.899	0.508	0.724	142.55
Pt/C	0.866	0.142	0.098	64.25

Table S2. lattice parameters of Pt (111), PtP_2 (111) and Pt/PtP_2 (111)

Sample	a（Å）	b（Å）	α（°）	β（°）	γ（°）
Pt	8.41940	8.41940	90.000	90.000	120.0000
PtP_2	8.12620	8.12620	90.000	90.000	120.0000

Table S3. ORR activity comparasion of core-shell structure in acid environment from previous literatures.

Sample	Mass activity (A/mg_{Pt})	Specific activity （mA/cm^2）	Ref
Core-shell Pt/PtP_2	0.685	1.35	This work
Core-shell-like Pt_3Co		0.14	[5]
Ti−Au@Pt/C	3.0	1.32	[6]
Pd–Pt Core–Shell	2.66	3.31	[7]
Co@Pt core-shell	0.17	0.41	[8]
$Pt_{ML}/AuNi_{0.5}Fe$	0.18	1.12	[9]
Core-shell Ni/Pt	0.49	1.95	[10]
Core-Shell Pt-Cu		0.45	[11]

1. C. B. Krishnamurthy, O. Lori, L. Elbaz and I. Grinberg, *J. Phys. Chem. Lett.*, 2018, **9**, 2229-2234.
2. A. Holewinski, J. C. Idrobo and S. Linic, *Nat. Chem.*, 2014, **6**, 828-834.
3. J. Li, H.-M. Yin, X.-B. Li, E. Okunishi, Y.-L. Shen, J. He, Z.-K. Tang, W.-X. Wang, E. Yücelen, C. Li, Y. Gong, L. Gu, S. Miao, L.-M. Liu, J. Luo and Y. Ding, *Nat. Energy*, 2017, **2**, 17111.
4. S. T. Hunt, M. Milina, A. C. Albarubio, C. H. Hendon, J. A. Dumesic and Y. Romanleshkov, *Science*, 2016, **352**, 974-978.
5. J. Jang, J. Kim, Y. Lee, I. Y. Kim, M. Park, C. Yang, S. Hwang and Y. Kwon, *Energy Environ. Sci.*, 2011, **4**, 4947-4953.
6. J. Hu, L. Wu, K. A. Kuttiyiel, K. R. Goodman, C. Zhang, Y. Zhu, M. B. Vukmirovic, M. G. White, K. Sasaki and R. R. Adzic, *J. Am. Chem. Soc.*, 2016, **138**, 9294-9300.
7. Y. Xiong, H. Shan, Z. Zhou, Y. Yan, W. Chen, Y. Yang, Y. Liu, H. Tian, J. Wu and H. Zhang, *Small*, 2017, **13**, 1603423.
8. D. A. Cantane, F. E. R. Oliveira, S. F. Santos and F. H. B. Lima, *Appl. Catal. B*, 2013, **136-137**, 351-360.
9. K. Gong, D. Su and R. R. Adzic, *J. Am. Chem. Soc.*, 2010, **132**, 14364-14366.
10. S. Zhang, Y. Hao, D. Su, V. V. T. Doannguyen, Y. Wu, J. Li, S. Sun and C. B. Murray, *J. Am. Chem. Soc.*, 2014, **136**, 15921-15924.
11. X. Ge, L. Chen, J. Kang, T. Fujita, A. Hirata, W. Zhang, J. Jiang and M. Chen, *Adv. Funct. Mater.*, 2013, **23**, 4156-4162.